Eur. Phys. J. B **38**, 431–436 (2004)
DOI: 10.1140/epjb/e2004-00136-7

THE EUROPEAN PHYSICAL JOURNAL B

# Optical characterization of ferroelectric $Bi_{3.25}La_{0.75}Ti_3O_{12}$ thin films

Z.G. Hu[a], Z.M. Huang, Y.N. Wu, S.H. Hu, G.S. Wang, J.H. Ma, and J.H. Chu

National Laboratory for Infrared Physics, Shanghai Institute of Technical Physics, Chinese Academy of Sciences, 500 Yu Tian Road, Shanghai 200083, P.R. China

Received 10 April 2003 / Received in final form 25 February 2004
Published online 28 May 2004 – 

**Abstract.** Amorphous and crystalline $Bi_{3.25}La_{0.75}Ti_3O_{12}$ (BLT) thin films on vitreous silica and sapphire substrates are prepared from chemical solutions. Their optical properties are investigated by transmittance measurements at energies from 1.1 to 5.0 eV. A four-phase model consisting of air, surface rough layer, BLT, and substrate is used to simulate the measured transmittance spectra. The inverse synthesis method with a double Tauc-Lorentz (DTL) dispersion function is used to calculate the optical constants and film thicknesses. The dispersion of the refractive index in the transparent region agrees with Sellmeier's dispersion relation. The absorption edges of the BLT films are different in the amorphous and crystalline cases.

**PACS.** 78.20.Ci Optical constants (including refractive index, complex dielectric constant, absorption, reflection and transmission coefficients, emissivity) – 78.66.Nk Insulators – 78.68.+m Optical properties of surfaces – 78.40.Ha Other nonmetallic inorganics

## 1 Introduction

Ferroelectric thin films attract considerable attention owing to their wide range of applications such as high dielectric constant capacitors, dynamic random-access memories with low switching voltage, electro-optic devices, etc. [1,2]. Bismuth-based layer-structure compounds are among the most promising ferroelectric materials owing to their high dielectric constants, and excellent ferroelectric, piezoelectric, and electro-optic properties. Recently, thin films of these compounds gained considerable interest for a variety of integrated device applications such as optical memory and electro-optic ones [3–6]. Thin films offer the potential for increased speeds, reduced operating voltages, and enhanced efficiency. High optical transparency at visible wavelengths and high refractive index are essential parameters for optical devices [7]. Among such materials, $Bi_4Ti_3O_{12}$ and $Bi_{3.25}La_{0.75}Ti_3O_{12}$ (BLT) offer a unique combination of large remnant polarization, large electro-optical coefficient, and low processing temperatures. They are considered as very promising for integrated optic applications [8–10]. Moreover, BLT possesses excellent fatigue-resistance characteristics on metal electrodes, making it more competitive for future applications [11]. There are reports on the optical properties of $Bi_4Ti_3O_{12}$ and BLT thin films [12–15]. Recently, we investigated the relation between optical properties and BLT film thickness [16]. The optical properties reported so far are in the visible and near infrared regions, while no information is available in the ultraviolet because the optical constants were obtained with the envelope method [17]. Moreover, effects of the annealing temperature and of different substrates on the optical properties of the films are of interest for potential applications.

Transmittance and/or reflectance spectroscopy are among the usual methods to study the optical properties of films deposited on transparent or partly transparent substrates [17–20]. This approach is convenient and widely available compared to spectroscopic ellipsometry [21]. In this paper, the optical properties of BLT thin films deposited on vitreous silica and sapphire are investigated by transmittance spectroscopy at energies from 1.1 to 5.0 eV, i.e. at wavelengths from 1100 to 248 nm.

## 2 Experimental procedure

$Bi_{3.25}La_{0.75}Ti_3O_{12}$ thin films on vitreous silica and (0001) sapphire substrates were prepared by the chemical solution method. The starting materials are bismuth nitrate, lanthanum acetate, and titanium butoxide. Bismuth nitrate and lanthanum acetate are mixed in the molar ratio Bi:La=3.25:0.75, and dissolved in heated glacial acetic acid. An appropriate amount of acetylacetone is added to stabilize the solution. An equimolar amount of titanium butoxide is then added. The concentration of this

[a] e-mail: zm2hzg@hotmail.com

precursor solution is 0.05 M in BLT. The BLT films are deposited by spin coating onto the substrates at 3500 rpm for 30 s. Each layer is dried at 180 °C for 3 min, then prefired at 350 °C for 3 min to remove residual organics, then post-annealed at 675 °C for 3 min in air using a rapid thermal annealing process. The cycle is repeated in the same order until a crystalline thin film of nominal thickness 150 nm is obtained. For one sample on vitreous silica, the post-annealing process is skipped. Obviously, the thickness of this amorphous film is larger than that of post-annealed crystalline films. The preparation details are found in [16].

The crystalline structure of the films is analyzed by X-ray diffraction (XRD) using Cu-K$\alpha$ radiation. The optical transmission is recorded with a double beam ultraviolet-visible spectrophotometer (Perkin Elmer UV/VIS Lambda 2S) at wavelengths from 1100 to 248 nm in steps of 2 nm. The transmittance spectra of the uncoated substrates are also measured for comparison.

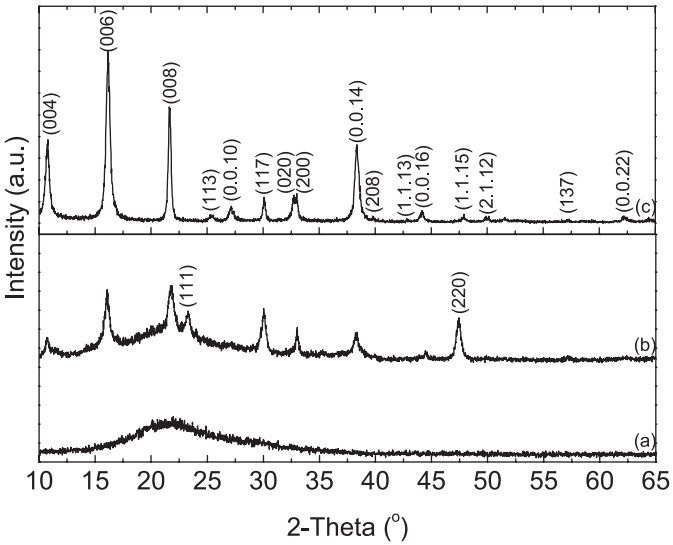


**Fig. 1.** X-ray diffraction patterns of BLT films: (a) amorphous on vitreous silica; (b) crystalline on vitreous silica; (c) crystalline on sapphire.

## 3 Results and discussion

### 3.1 Crystalline quality

Figure 1 shows the XRD patterns of BLT films deposited on vitreous silica and sapphire. The crystallization and grain orientation of the films strongly depend on annealing and on the substrate. The non-annealed BLT film is apparently amorphous (labeled A). The XRD patterns of the films annealed at 675 °C are different on vitreous silica and sapphire substrates. On vitreous silica the film is polycrystalline (labeled C) and it shows well-defined XRD peaks with no preferential orientation. On sapphire the film is polycrystalline (C) with $c$-axis orientation. The annealed films have the layered perovskite structure. The XRD pattern on sapphire shows more and sharper diffraction peaks than on vitreous silica. There is an obvious preferential orientation of the growing BLT crystallites on the crystalline sapphire substrate.

### 3.2 Physical model

The inverse synthesis method is based on a phenomenological model fitted to the experiment. The reliability of this method essentially depends on the validity of the model. A stack of films deposited on a substrate of finite thickness can be reduced to a system of two interfaces. The optical model for the calculation of the transmittance spectrum on transparent substrates is described in [22–24]. The dispersion is represented by the Tauc-Lorentz (TL) dispersion formula [25]. It is derived from the Tauc joint density of states and the standard Lorentz form for the imaginary part $\varepsilon_2$ of the complex dielectric function for a collection of oscillators. It has been successfully applied to many amorphous and crystalline materials [25–27]. The single TL dispersion function is

$$\varepsilon_2(E) = \begin{cases} \dfrac{AE_0C(E-E_g)^2}{(E^2-E_0^2)^2+C^2E^2}\dfrac{1}{E}, & (E > E_g) \\ 0 \quad (E \le E_g). \end{cases} \tag{1}$$

The real part $\varepsilon_1$ is obtained using the Kramers-Kronig relation,

$$\varepsilon_1(E) = \varepsilon_\infty + \frac{2}{\pi}P\int_{E_g}^{\infty}\frac{\xi\varepsilon_2(\xi)}{\xi^2-E^2}d\xi. \tag{2}$$

Equations (1) and (2) depend on five parameters: the transition matrix element $A$, the peak transition energy $E_0$, the broadening term $C$, the band gap energy $E_g$, and the high-frequency dielectric constant $\varepsilon_\infty$. The appropriate value of $\varepsilon_\infty$ depends on the dispersion model which is used at lower energies and it is not known a priory. Fitting the results obtained for the C-film on vitreous silica we find $\varepsilon_\infty = 1.30$. The correlation coefficient between $\varepsilon_\infty$ and the other parameters is the smallest for this particular film. Therefore, $\varepsilon_\infty$ is fixed to this value for all films in order to decrease the number of free parameters and to improve the comparison between the different films. We find that a double TL-dispersion function (DTL) is necessary to describe with sufficient accuracy the optical dispersion of the BLT films.

We adopt a four-phase model consisting of air, surface rough layer, BLT, and substrate, all assumed optically isotropic. Bruggeman effective medium approximation [28] is used to calculate the effective dielectric function of the rough layer which is assumed to consist of 50% BLT and 50% voids of refractive index unity. The parameters of the fit are the two layer thicknesses and the $4 \times 2$ dispersion-relation variables. The optical constants of the

substrates were calculated from their transmittance spectra [20]. There are slight differences between these calculated values and tabulated ones [29] which do not affect the final results.

The least-square procedure employed is the modified Levenberg-Marquardt algorithm. The fit quality is measured by the deviation$\sigma$ defined by

$$\sigma^2 = \frac{1}{N-M}\sum_{i=1}^{N}\left(\frac{T_i^m - T_i^c}{\sigma_{T,i}}\right)^2, \qquad (3)$$

where $T_i^c$ and $T_i^m$ are the calculated and measured values at the $i$th data point and $\sigma_{T,i}$ is the measurement error at that wavelength. $N$ is the number of wavelength values and $M$ is the number of free parameters.

### 3.3 Optical properties

Typical transmittance spectra of the films and substrates are shown in Figure 2. The spectra can roughly be divided in two regions: a transparent oscillating one and a strongly absorbing one at higher energies. The absorption edge corresponds to the end of the interference oscillations. The transmittance spectra of A and C-BLT films on vitreous silica are different, as seen from Figures 2a and b. Both the transparent region and the oscillation peaks move to higher energies in going from A to C. This indicates that the film optical thickness decreases and that the band gap increases with annealing. The transmission in the transparent oscillating region of the A film is also higher than for the C film, indicating that the refractive index is larger for the latter.

The best fits to the transmittance data are shown by dotted lines in Figure 2. These are hardly distinguishable from the measured values. The deviations $T_m$-$T_c$ are plotted on an expanded scale in Figure 3. The ten fitting parameters and their 90% confidence limits are listed in Table 1. Figure 2 shows that the model represents reasonably well the measured data although it is not perfect as seen from Figure 3. The main difficulty occurs near the gap which is steeper in the model than in reality. A second difficulty is in the rather ad hoc choice of a single TL dispersion to represent the dielectric properties at long wavelengths (the first TL parameters in Tab. 1). However, the mean-square deviations $\sigma$ listed in the table are sufficiently small to guarantee that the accuracy of the complex dielectric function is within about 2% over the fitted range. The fitted total thicknesses, which are the sum of the surface rough layer and BLT film thicknesses, agree with values measured by a Rank Tallystep profiler. This also supports the validity of the method. The surface rough layer of the A-BLT film is smaller than that of C films. Moreover, the surface rough layer on sapphire is larger than on vitreous silica. This may be due to the size of crystalline grains and their interactions during the post-annealing process.

The calculated refractive indices $n$ and extinction coefficients $\kappa$ in function of energy are shown in Figure 4. The refractive indices on vitreous silica increase slowly, and reach a maximum beyond which they gradually fall with further increase of $E$. The refractive index of the BLT film on sapphire increases slowly, it experiences an oscillation around 4.2 eV, and it further increases gradually with $E$. At 1.96 eV (typical energy of the He-Ne laser), the refractive indices of the BLT films on vitreous silica are 2.14

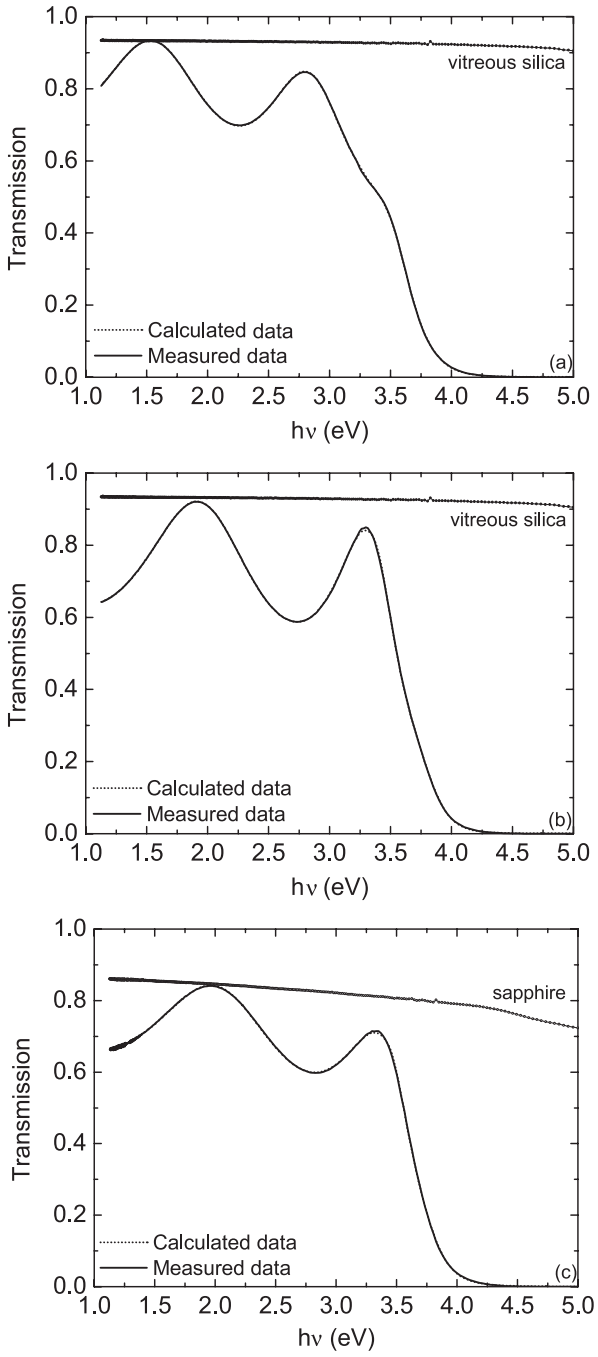


**Fig. 2.** Transmittance spectra of BLT films and their fits: (a) amorphous on vitreous silica; (b) crystalline on vitreous silica; (c) crystalline on sapphire.

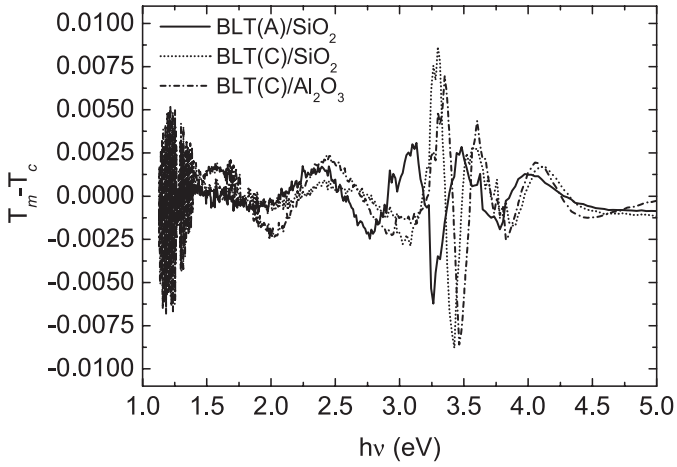


**Fig. 3.** Deviations between measured and calculated transmission values.

**Table 1.** Parameter values of the DTL model used in fitting the optical functions of the BLT films. The 90% confidence limits are indicated. Notation: "BLT(A)/$SiO_2$" represents the amorphous BLT film on vitreous silica; "BLT(C)/$SiO_2$" represents the crystalline BLT film on vitreous silica; "BLT(C)/$Al_2O_3$" represents crystalline BLT film on sapphire; $E_0$ and $E_d$ are Sellmeier dispersion parameters; $t_s$ and $t_f$ are the thicknesses of the surface rough layer and the BLT films, respectively.

| Samples | BLT(A)/$SiO_2$ | BLT(C)/$SiO_2$ | BLT(C)/$Al_2O_3$ |
|---|---|---|---|
| $A_1$ (eV) | $18.6 \pm 0.4$ | $16.7 \pm 3.0$ | $18.4 \pm 1.3$ |
| $E_{g1}$ (eV) | $1.22 \pm 0.02$ | $0.48 \pm 0.08$ | $0.79 \pm 0.03$ |
| $E_{01}$ (eV) | $6.38 \pm 0.05$ | $6.03 \pm 0.25$ | $5.51 \pm 0.06$ |
| $C_1$ (eV) | $0.78 \pm 0.04$ | $0.37 \pm 0.03$ | $0.50 \pm 0.03$ |
| $A_2$ (eV) | $82.2 \pm 2.5$ | $190.9 \pm 6.8$ | $292.6 \pm 19.7$ |
| $E_{g2}$ (eV) | $3.20 \pm 0.01$ | $3.37 \pm 0.01$ | $3.44 \pm 0.01$ |
| $E_{02}$ (eV) | $4.09 \pm 0.01$ | $4.10 \pm 0.01$ | $3.88 \pm 0.02$ |
| $C_2$ (eV) | $1.60 \pm 0.04$ | $1.38 \pm 0.03$ | $1.45 \pm 0.07$ |
| $t_s$ (nm) | $21.0 \pm 0.5$ | $24.2 \pm 0.3$ | $27.4 \pm 0.2$ |
| $t_f$ (nm) | $183.6 \pm 0.4$ | $120.8 \pm 0.2$ | $110.0 \pm 0.2$ |
| $E_0$ (eV) | 5.69 | 5.58 | 5.39 |
| $E_d$ (eV) | 18.06 | 25.55 | 26.62 |
| $\sigma$ | 0.0963 | 0.1216 | 0.2018 |

and 2.49 for the A and C films, respectively. On sapphire the index takes the larger value 2.59. For the A film, the density is lower than for C ones, which may explain the lower refractive index and higher transmission. The refractive indices of the present C-BLT films are larger than the value 2.26 observed on Pt/Ti/$SiO_2$/Si substrates [16].

For insulators, the refractive index dispersion in the transparent region can usually be represented by Sellmeier's equation [30],

$$n^2(E) - 1 = \frac{E_0 E_d}{E_0^2 - E^2}, \quad (4)$$

where $E_0$ is the single electronic oscillator energy and $E_d$ is the dispersion energy. For many dielectrics, the dispersion energy can be used to evaluate the electro-optical and nonlinear optical constants of thin films [30]. We plot

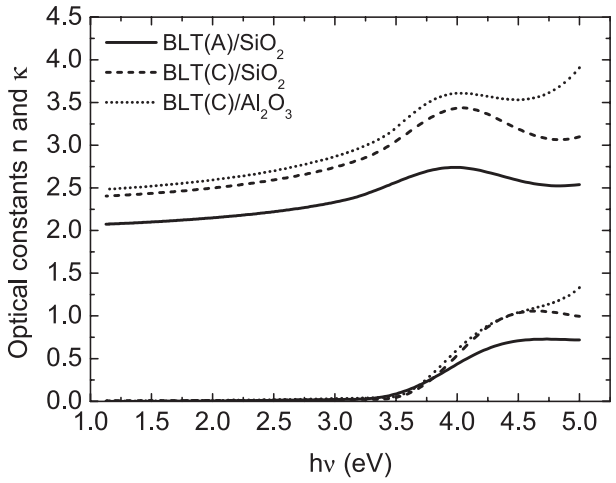


**Fig. 4.** Refractive indices $n$ and extinction coefficients $\kappa$ of the BLT films in function of energy: "BLT(A)/$SiO_2$" is for the amorphous film on vitreous silica, "BLT(C)/$SiO_2$" for the crystalline film on vitreous silica, and "BLT(C)/$Al_2O_3$" for the crystalline film on sapphire.

$(1/(n^2-1))$ vs. $(h\nu)^2$ for the BLT films in Figure 5. The data fit to straight lines indicating the applicability of Sellmeier's formula. The different values of $E_0$ and $E_d$ estimated from these plots are listed in Table 1. One notes that these parameters depend on substrate and annealing. The $E_0$ values of the annealed films are also larger than the value 5.29 eV obtained on Pt/Ti/$SiO_2$/Si substrates [16]. It was reported that $E_0$ for $Bi_4Ti_3O_{12}$ films is 4.77 eV [13]. The variations of $E_0$ may be due to different substrates and crystalline qualities. From the XRD patterns (Fig. 1), the crystalline characteristics of the BLT films on vitreous silica and sapphire are different which can affect the optical properties of the films. The thermal mismatch strains in BLT films on vitreous silica and sapphire are different owing to differences in thermal expansion coefficients [20,31]. The (006) $d$-spacings are 5.5140 and 5.4803 Å on vitreous silica and sapphire, respectively. For BLT powder, $d$ is 5.4733 Å [32]. Obviously, there are mismatch strains in BLT films. We believe that changes in optical constants are mainly due to the crystalline quality, the thermal mismatch strains, and the annealing temperature.

The extinction coefficients $\kappa$ are nearly zero in the interference region. On vitreous silica, $\kappa$ increases rapidly with $E$, reaches a maximum, and falls slightly at higher energies. On sapphire, $\kappa$ increases in the transparent region to a maximum value with increasing photon energy (see Fig. 4). Near the fundamental band gap energy, $\kappa$ is not zero because of defects and disorder in the films [31]. We note a point of inflection in the extinction coefficient curves, where the rate of increase of the coefficient slows down. This agrees with observations on BST thin films of different thicknesses [33], and also on Ti oxide films [34].

The absorption coefficient $\alpha$ of the films is calculated from $\alpha = 4\pi k/\lambda$. Figure 6 shows $\alpha$ in function of the energy $h\nu$. The values near the band gap are displayed in the inset of Figure 6. This suggests that the absorption edge might be different for the different films. It was

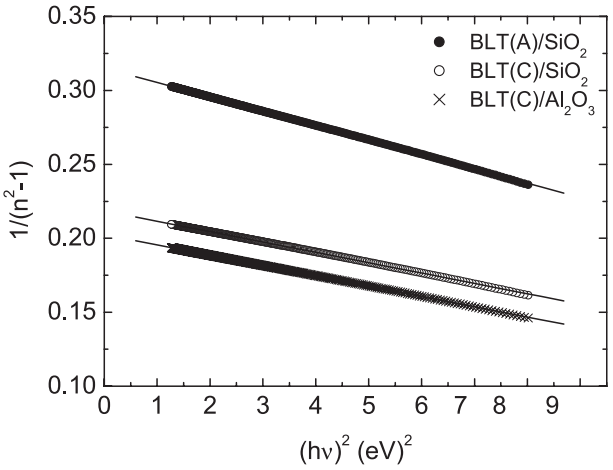


**Fig. 5.** Experimental values (dotted lines) and single electronic oscillator model (solid lines) in function of $(h\nu)^2$ for various BLT films.

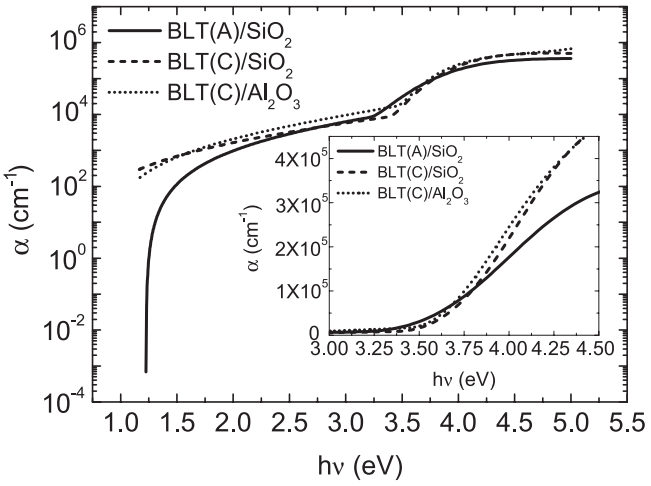


**Fig. 6.** Semi-logarithmic presentation of the absorption coefficient $\alpha$ in function of the photon energy for BLT films. The inset shows $\alpha$ near the absorption edge.

reported that the gap energy of BLT films on $Pt/Ti/SiO_2/Si$ is 3.25 eV [15], lower than the present values since $\alpha$ is here nearly zero at 3.25 eV. It was also reported that the gap energy of $Bi_4Ti_3O_{12}$ films decreases with increasing annealing temperature [12,14] and these values are also lower than found here. Note that the surface rough layer was taken into account here and that this may induce differences in the position of the absorption edge. We believe that the crystallinity of the films leads to changes in the absorption edge. It is broader for A-BLT than for C-BLT. This indicates that there are more defects in A-BLT. On the other hand, the fitting parameters $E_{g2}$ are $3.20 \pm 0.01$, $3.37 \pm 0.01$, and $3.44 \pm 0.01$ eV for A-BLT/$SiO_2$, C-BLT/$SiO_2$, and C-BLT/$Al_2O_3$, respectively. Fixing $E_{g2}$ to 3.40 eV, quite satisfactory fits are also obtained for both C films [35]. It seems however that the crystalline films have a larger band gap than the amorphous one.

## 4 Conclusions

In conclusion, amorphous and crystalline $Bi_{3.25}La_{0.75}Ti_3O_{12}$ thin films on vitreous silica and sapphire substrates were prepared by the chemical solution method. The optical properties of the BLT films on vitreous silica and sapphire have been investigated by transmittance measurements in the energy range from 1.1 to 5.0 eV. The inverse synthesis method was used to calculate the optical constants and film thicknesses. The fitted thickness values for the three samples are 184, 121, and 110 nm, for A-BLT/$SiO_2$, C-BLT/$SiO_2$, and C-BLT/$Al_2O_3$, respectively. The corresponding surface rough layer thicknesses are 21, 24, and 27 nm, respectively. The dispersion of the refractive index in the transparent region is represented successfully in terms of a single electronic oscillator of energy 5.69, 5.58, and 5.39 eV, and dispersion 18.1, 25.6, and 26.6 eV, respectively. In the interference region, the extinction coefficients of the BLT films are nearly 0. Our results indicate that a double Tauc-Lorentz dispersion function is fairly satisfactory to fit the optical constants of BLT films. Finally, the absorption edge seems different between the amorphous and crystalline films, crystalline films having a larger band gap.

This work was supported by the special funds for Major State Basic Research Project No.G001CB3095 of China and by the National Science Foundation in China No.60223006 and No.60221502.

## References

1. B.H. Park, B.S. Kang, S.D. Bu, T.W. Noh, J. Lee, W. Jo, Nature (London) **401**, 682 (1999)
2. Y.H. Xu, J.D. Mackenzie, Integrated Ferroelectrics **1**, 17 (1992)
3. H.N. Lee, D. Hesse, N. Zakharov, U. Gösele, Science **296**, 2006 (2002)
4. K. Kato, K. Suzuki, K. Nishizawa, T. Miki, Appl. Phys. Lett. **78**, 1119 (2001)
5. K.M. Satyalakshmi, M. Alexe, A. Pignolet, N.D. Zakharov, C. Harnagea, S. Senz, D. Hesse, Appl. Phys. Lett. **74**, 603 (1999)
6. A. Kingon, Nature (London) **401**, 658 (1999)
7. S.B. Majumder, M. Jain, R.S. Katiyar, Thin Solid Films **402**, 90 (2002)
8. Y. Hou, X.H. Xu, H. Wang, M. Wang, S.X. Shang, Appl. Phys. Lett. **78**, 1733 (2001)
9. A.Q. Jiang, Z.X. Hu, L.D. Zhang, Appl. Phys. Lett. **74**, 114 (1999)
10. Y. Shimakawa, Y. Kubo, Y. Tauchi, H. Asano, T. Kamiyama, F. Izumi, Z. Hiroi, Appl. Phys. Lett. **79**, 2791 (2001)
11. M.W. Chu, M. Ganne, M.T. Caldes, L. Brohan, J. Appl. Phys. **91**, 3178 (2002)
12. H.S. Gu, D.H. Bao, S.M. Wang, D.F. Gao, A.X. Kuang, XJ. Li, Thin Solid Films **283**, 81 (1996)

13. M. Yamaguchi, T. Nagamoto, O. Omoto, Thin Solid Films **300**, 299 (1997)
14. X.S. Wang, J.W. Zhai, L.Y. Zhang, X. Yao, Infrared Physics and Technology **40**, 55 (1999)
15. G.S. Wang, X.J. Meng, Z.Q. Lai, J. Yu, J.L. Sun, S.L. Guo, J.H. Chu, Appl. Phys. A **76**, 83 (2003)
16. Z.G. Hu, G.S. Wang, Z.M. Huang, J.H. Chu, J. Appl. Phys. **93**, 3811 (2003)
17. R. Swanepoel, J. Phys. E: Sci. Instrum. **16**, 1214 (1983)
18. J.C. Manifacier, J. Gasiot, J.P. Fillard, J. Phys. E **9**, 1002 (1976)
19. C.H. Peng, S.B. Desu, J. Am. Ceram. Soc. **77**, 929 (1994)
20. Z.G. Hu, Z.M. Huang, Z.Q. Lai, G.S. Wang, J.H. Chu, Thin Solid Films **437**, 223 (2003)
21. R. Ferrini, G. Guizzetti, M. Patrini, A. Parisini, L. Tarricone, B. Valenti, Eur. Phys. J. B **27**, 449 (2002)
22. *Optical Properties of Thin Solid Films*, edited by O.S. Heavens (Dover, New York, 1965)
23. D. Davazoglou, Appl. Phys. Lett. **70**, 246 (1997)
24. D. Davazoglou, Thin Solid Films **302**, 204 (1997)
25. G.E. Jellison Jr, F.A. Modine, Appl. Phys. Lett. **69**, 371 (1996); G.E. Jellison Jr, F.A. Modine, Appl. Phys. Lett. **69**, 2137 (1996)
26. Y.J. Cho, N.V. Nguyen, C.A. Richter, J.R. Ehrstein, B.H. Lee, J.C. Lee, Appl. Phys. Lett. **80**, 1249 (2002)
27. G.E. Jellison Jr, Thin Solid Films **234**, 416 (1993)
28. D.E. Aspnes, A.A. Studna, E. Kinsbron, Phys. Rev. B **29**, 768 (1984)
29. *Handbook of Optical Constants of Solids*, edited by E.D. Palik (Academic Press, New York, 1985)
30. M. DiDomenico Jr, S.H. Wemple, J. Appl. Phys. **40**, 720 (1969)
31. V. Srikant, D.R. Clarke, J. Appl. Phys. **81**, 6357 (1997)
32. B. Aurivillius, Ark. Kemi **1**, 499 (1949)
33. Z.G. Hu, G.S. Wang, Z.M. Huang, X.J. Meng, F.W. Shi, J.H. Chu, Jpn J. Appl. Phys. **42**, 1400 (2003)
34. S.Y. Kim, Appl. Opt. **35**, 6703 (1996)
35. When this is done, the parameters in Table 1 are changed beyond the indicated errors bars, except for the thicknesses. The largest changes occur for the oscillator strengths